IOPscience iopscience.iop.org

Home Search Collections Journals About Contact us My IOPscience

A computer simulation study of the disorder in ammonium perrhenate

This article has been downloaded from IOPscience. Please scroll down to see the full text article.

1994 J. Phys.: Condens. Matter 6 9903

(http://iopscience.iop.org/0953-8984/6/46/010)

View the table of contents for this issue, or go to the journal homepage for more

Download details:
IP Address: 171.66.16.151
The article was downloaded on 12/05/2010 at 21:06

Please note that terms and conditions apply.

J. Phys.: Condens. Matter 6 (1994) 9903–9928. Printed in the UK

A computer simulation study of the disorder in ammonium perrhenate

R J C Brown† and R M Lynden-Bell
University Chemical Laboratory, Lensfield Road, Cambridge CB2 1EW, UK

Received 1 July 1994

Abstract. Ammonium scheelites (of which ammonium perrhenate is an example) show several anomalies in their behaviour (including thermal contraction of the a lattice parameter, large thermal expansion of the c lattice parameter, enhanced nuclear quadrupolar relaxation, increased specific heat) which has been attributed to the onset of orientational disorder of the ammonium ions. Unlike in the ammonium halides there is no actual phase transition. Extensive molecular dynamics simulations of this material are reported. The model shows anomalies in the thermal expansion which are associated with a broadening and shift of the orientational distribution of the ammonium ions. There is no evidence of more than one preferred orientation. The ammonium ions also begin to jump between the twelve equivalent orientations, and we present evidence that this is primarily by rotation about one of the bonds. The activation energy for this agrees well with experiment. Angular and linear velocity–time correlation functions for the ammonium ion show rapid dephasing at higher temperatures, which is consistent with the observed broadening of the corresponding lines in the Raman spectrum. The origin of the anomalous thermal expansion is discussed in terms of various contributions to the entropy of the crystal.

1. Introduction

1.1. Ammonium scheelites and their peculiarities

The ammonium scheelites are ionic materials of composition NH_4MX_4 consisting of an ammonium ion and a tetrahedral anion and having the scheelite ($CaWO_4$) structure. Examples are ammonium perrhenate, ammonium metaperiodate and ammonium pertechnetate. The scheelite structure (see figure 1) has a tetragonal unit cell with four formula units per crystallographic unit cell. At low temperatures both types of ion occupy well defined orientations with only small-amplitude librations about positions of minimum energy [1]. At high temperatures the ammonium ion (or its deutero-analogue) begins to rotate rapidly and the crystal lattice shows anomalous expansion. This change is reminiscent of the phase transition from a normal crystalline phase to an orientationally disordered phase (sometimes known as a rotator phase) seen in alkali metal cyanides and ammonium halides. In these crystals the site symmetry at the molecular ion is higher in the phase in which the ion is disordered and is incompatible with the the molecular symmetry of the ion. Thus the space group of the crystal changes at the order–disorder phase transition. In the ammonium scheelites, however, there is no change in the symmetry of the crystal structure and no actual order–disorder phase transition, so we describe the changes simply as a disordering process.

† Permanent address: Department of Chemistry, Queen's University, Kingston, Ontario K7L 3N6, Canada.

0953-8984/94/469903+26$19.50 © 1994 IOP Publishing Ltd

The cation site in the scheelites has S_4 symmetry in both potassium [2] and ammonium salts, so it is not surprising that replacing the T_d NH_4^+ ion by a spherical average does not cause a phase change. However, there are changes in the properties of NH_4ReO_4 which are clearly associated with increasing freedom of movement of the ammonium ions above about 100 K. These are: firstly the unit cell contracts in the *a* direction and expands more than expected in the *c* direction; secondly, there is additional contribution to the specific heat [3, 4]; thirdly, neutron diffraction shows that the average orientation of the ND_4^+ ions changes and the thermal ellipsoid elongates [1]; fourthly, the NH_4^+ lines in the Raman spectrum broaden and disappear [5, 6]. NMR relaxation time measurements indicate that the ammonium ions are reorienting rapidly except at very low temperatures [7]. The temperature and pressure coefficients of the NQR frequency are both positive between about 100 K and 400 K [8].

These observations show that not only has the ammonium ion become more mobile, but also the material has gained additional entropy. It is tempting to equate this entropy gain to an additional orientational disorder of the ammonium ions, which in turn drives the elongation of the unit cell. Taylor [9, 10] proposed a two-site spin model for the ammonium-ion orientation, and showed that this could account for many of the experimental observations. In this model the two sites have unequal probabilities and the entropy gain arises from increased population of the less favourable site. An alternative approach [4] is to associate the entropy increase with the lattice strain and the change in ammonium-ion orientation as a consequence of the change in cell size.

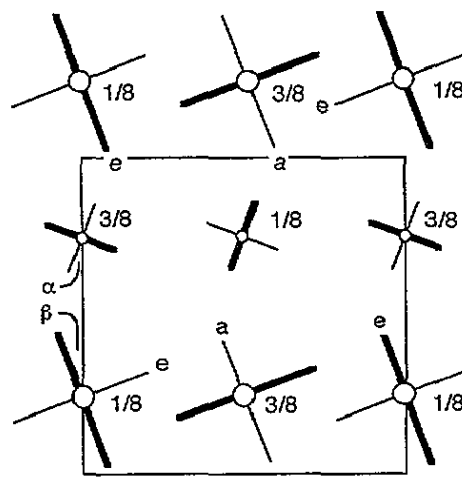

Figure 1. View of a projection of the bottom half of the scheelite unit cell along the *c* axis. The thin lines show the unit cell with its origin at an inversion centre. The large tetrahedra represent ReO_4^- ions and the small tetrahedra NH_4^+ ions. Note the upright and inverted configurations of each type of ion.

In this paper we report an extensive study of a model of ammonium perrhenate using computer simulation. Although we use the term 'model' in connection with both the Taylor spin model and with the current work, we should emphasize that the modelling in the two cases is at a different level. In the former work the aim was to describe the basic physics of the material in a very simple way. In the current work our aim is to provide a realistic microscopic description of the the material in order to investigate the causes of the thermal

changes and to justify (or not) simple models such as the spin model. But, as in all computer simulations, we study a model of the material rather than the material itself. We have to specify the intermolecular potential; in section 2.1 we shall describe our intermolecular potential and how we chose the parameters.

The model is not perfect, but does show most of the experimental features. At about 150 K the c axis begins to expand anomalously while the a axis contracts. The average orientation of the ND_4 ions changes and they begin to reorient on a time scale which decreases from about 10 ps at 220 K to about 0.5 ps at 420 K.

We shall show that there is no evidence for two preferred sites (as postulated in the spin model), but rather ions have a single preferred orientation whose orientation in the unit cell changes as the temperature is raised. The dynamics is consistent with jumps between equivalent sites by C_3 rotation about a randomly chosen ND bond. It is not consistent with small-angle diffusion.

We shall give a physical argument which explains why the a and c axes should change in this characteristic way when the average ammonium-ion orientation changes. However, the driving force for this change is not readily pinpointed. It is only partly due to increased orientational entropy of the cations and there is a significant contribution from increased translational freedom.

2. Details of the potential model and the simulation

2.1. The crystal structure

In the scheelite structure, part of which is shown in figure 1, there are four ions of each type in the unit cell (twice as many as in the primitive unit cell). Crystallographically the set of cations and the set of anions occupy Wyckoff b and a sites respectively. Each T_d ion is at a site of S_4 symmetry with one of its S_4 axes parallel to the z direction along the crystal c axis. The angle of rotation about this axis is not determined by symmetry, so there are two angles to be specified, α, which determines the orientation of the ammonium ions and β, which determines the perrhenate-ion orientation.

Figure 1 shows two layers of a unit cell and parts of its neighbours viewed down the c axis. The origin of the unit cell (outlined) is at a centre of inversion. The large tetrahedra in the top and bottom rows of this figure represent the perrhenate ions which are in the two two possible orientations in the layers at $c/8$ and $3c/8$. The smaller tetrahedra in the middle row of the figure represent NH_4^+ ions. These ions are in two types of site related by centres of symmetry. We shall use the terms 'upright' and 'inverted' to distinguish these sites. The mean orientations of the ions in these sites are also inverted. This is shown in the middle row of ions in the figure, which are (from left to right) in upright, inverted and upright sites. The angle α defines the orientation of one type of site; the corresponding angle for the inverted site is $90°+\alpha$. ReO_4^- ions also occupy upright and inverted sites (see the bottom row of the figure) and the angle α is defined as shown for an upright site; again the same relationship between the orientations of the ReO_4^- ions in the two types of site holds.

We shall have occasion to refer to the oxygen atoms which are in 'axial' and 'equatorial' positions relative to a particular ammonium ion. These are almost equidistant from the centre of the cation site, with the axial oxygen atoms being slightly nearer. They are marked in the figure for the ammonium ion in the centre of the figure. Note that at low temperatures the ND bonds point towards the axial oxygen atoms. These are on the nearest perrhenate

ions in the planes above and below (the latter are not shown). In order to point to the equatorial oxygen atoms, which are on ions in the same plane, the ammonium ions would have to rotate from $\alpha \approx 13°$ to $\alpha \approx -50°$ about the c axis.

Table 1. Potential parameters.

Atoms	$A_{ij}/10^5\,\mathrm{kJ\,mol^{-1}}$	$\sigma_{ij}/\text{Å}$
O–O	2.34	4.18
O–N	2.30	3.7136
O–D	2.00	5.70
N–N	2.30	3.42
$q_O = -0.5808\,e$		$q_D = 0.469\,e$
$q_{Re} = 1.3232\,e$		$q_N = -0.876\,e$

2.2. *The potential*

We require a potential which is quick to compute but which is sufficiently detailed to provide a realistic model. As in earlier work on crystals with molecular ions [11, 12], we use rigid ions with charges on each atom, plus atom–atom repulsive terms between atoms on different ions. Thus

$$V = \sum_{i<j} \left\{ \frac{q_i q_j e^2}{4\pi\epsilon_0 r_{ij}} + A_{ij} \exp(-\rho_{ij} r_{ij}) \right\}. \tag{1}$$

The values of the parameters used are given in table 1. The total charge on on each ion was taken to be $\pm e$. The ND_4^+ atomic charges were chosen to give the octopole moment calculated by Fowler *et al* [13], while the ReO_4^- atomic charges were almost the same as we fitted in preliminary work on the potassium salt [14]. The significant interatomic repulsions were assumed to be D–O, N–O and O–O. N–N repulsions were included but make only a small contribution to the energy. No explicit D–D repulsion was included apart from the electrostatic repulsion. As the rhenium atoms are buried in a shell of oxygens, all non-coulombic interactions involving rhenium were taken to be zero. Each ion was modelled as a rigid tetrahedron with bond lengths $r_{ND} = 1.025$ Å and $r_{ReO} = 1.739$ Å. The chief defect of this model is probably the lack of polarizability in the perrhenate ion.

The potential parameters were adjusted so as to give zero xx and zz stresses at a temperature of 20 K with the unit cell dimensions set equal to their experimental values [1]. The main adjustments were to the oxygen-atom charge and the oxygen–cation repulsive term. In the case of the ammonium salt, there is also the question of the relative strengths of the O–D and O–N repulsive terms, which at higher temperatures influences the energy barrier to rotation. In all, four sets of potential parameters were examined, and one chosen for detailed study. The criteria for selection were (a) the prediction of negative a-axis thermal expansion, (b) reasonable temperature dependence of the angle β. One potential function failed on the first, and two others on the second criterion. The values of the structural parameters determined using the potential defined by the numbers in table 1 are given in table 2.

Table 2. Temperature and pressure dependence of structural properties of the model. The lattice parameters are determined to approximately ±0.1%; the pressures to ±0.1 kbar and the lattice energies to ±0.1 kJ mol^{-1}

T/K	P/kbar	U/kJ mol^{-1}	a/Å	c/Å	β	α	$\bar{Q}$	α_Q
20	0	−604.4	5.999	12.39	29.8	13.2	0.98	13.1
120	0	−594.1	6.008	12.47	28.6	12.2	0.87	12.1
220	0	−583.0	6.002	12.62	27.1	9.2	0.73	9.3
320	0	−571.3	5.976	12.85	25.5	4.0	0.56	5.0
400	0	−561.9	5.976	13.02	23.7	0.0	0.46	2.6
420	0	−559.5	5.976	13.07	23.2	1.0	0.44	2.1
470	0	−553.3	5.976	13.19	20.5		0.38	0.8
420	5	−561.0	5.864	12.97	26.1	−1.5	0.41	−1.6
420	10	−561.8	5.786	12.86	27.9	−3.7	0.40	−4.6
420	20	−560.2	5.701	12.63	30.2	−5.2	0.41	−7.2
420	48	−549.0	5.56	12.10	34.7	−6.8	0.46	−9.8
420	(6.5)[a]	−562.2	5.999	12.39	27.4	4.9	0.5	6.2
420[b]	0	−559.3	5.976	13.07	23.1	0.9	0.43	1.6
420[c]	0	−559.3	5.976	13.07	23.2		0.43	1.9

[a] Run with zero-temperature cell. $p_{xx} = 4.0$ kbar, $p_{zz} = 11.7$ kbar.
[b] Run with NH_4^+ rather than ND_4^+.
[c] Run with NHD_3^+ rather than ND_4^+.

2.3. *Computer simulation*

Computer simulations were carried out on the deutero-ammonium salt using the method of molecular dynamics [15]. The program was the same as used previously [11, 12] and could be run under conditions of constant energy or temperature (using a Nosé thermostat) and constant cell size and shape or constant stress (using a Parrinello–Rahman barostat). Most runs were performed at constant temperature and pressure, but dynamical information was taken from runs at constant volume and temperature. The molecular dynamics cell contained 128 formula units arranged as $4 \times 4 \times 2$ unit cells. The unit cell is tetragonal and this structure was stable in all the constant-pressure runs. A time step of 5 fs was used. Data were usually collected from runs of 6000 time steps (30 ps) after equilibration at the appropriate temperature and volume or pressure.

2.4. *Analysis of results*

During each run the energy, cell parameters and mean orientation of both ammonium and perrhenate ions were monitored together with two orientational order parameters defined below. Where relevant, averages were taken separately over upright and inverted sites.

One property of particular interest is the orientational distribution of the ammonium ions; we used two methods of characterizing this. The first method was to monitor the order parameters Q_1 and Q_2 based on the $L = 3$ rotator functions [16]. The reason for using $L = 3$ rotator functions is that the lowest allowed spherical tensor for a tetrahedral molecule with T_d symmetry has $L = 3$. In terms of cartesian components the only non-vanishing term of such a third-rank tensor is XYZ if the axes are chosen along the S_4 axes of the ion, that is bisecting the bond angles. The site symmetry, however, is lower (S_4) and there are two $L = 3$ spherical harmonics which transform as the totally symmetric irreducible representation, namely xyz and $z(x^2 - y^2)$. Here the z axis is along the S_4 axis of the site, parallel to the c axis of the crystal, and the x axis is parallel to the crystal a axis.

The $L = 3$ rotator functions which are totally symmetric under the symmetry operations of both site and molecule are constructed from triple products of direction cosines between the X, Y and Z axes and x, y and z axes. All possible permutations of the molecular vectors (X, Y and Z) with the two A_1 combinations of the site vectors xyz and $z(x^2 - y^2)$ must be included, giving

$$Q_1 = X_x(Y_yZ_z + Z_yY_z) + Y_x(Z_yX_z + X_yZ_z) + Z_x(X_yY_z + Y_yX_z) \tag{2}$$

$$Q_2 = X_z(Y_xZ_x - Y_yZ_y) + Y_z(Z_xX_x - Z_yX_y) + Z_z(X_xY_x - X_yY_y) \tag{3}$$

where X_y is instantaneous value of the direction cosine between the X axis of the ion and the y axis of the crystal. The order parameters are the averages of these quantities calculated separately for upright and inverted sites. Note that the signs of the order parameters of the two sites are reversed as the sites are related by inversion of the molecular axes.

How can these order parameters be interpreted? If the orientational distribution were totally uniform, the values of both these order parameters would be zero. If there is a unique orientation, compatibility of the site and molecular symmetry requires that one of the S_4 axes of the ion must be along the c axis. In this case $Q_1^2 + Q_2^2 = 1$ and

$$Q_1 = \sin 2\alpha \qquad Q_2 = \cos 2\alpha. \tag{4}$$

We combine the calculated order parameters $\langle Q_2 \rangle$ and $\langle Q_1 \rangle$ into a single complex quantity

$$\langle Q_2 \rangle + \mathrm{i}\langle Q_1 \rangle = \bar{Q}\mathrm{e}^{2\mathrm{i}\alpha_Q} \tag{5}$$

where we can interpret $\bar{Q}$ as a measure of the total orientational order and α_Q as some average of the orientational angle α. $\bar{Q}$ is the same for upright and inverted sites, but α_Q changes sign on inversion. We quote the averages of α_Q for upright sites and $-\alpha_Q$ for inverted sites.

A more direct display of the orientational distribution was made by constructing contour plots of the probability of finding the orientation of the ND bond directions at different angles (θ, ϕ) relative to the crystal axes. Again upright and inverted sites must be treated separately. Imagine the probability distribution function of the bond orientations defined on a unit sphere. In order to represent this on a flat surface we used an equal-area projection [17] of the upper half of the sphere defined by

$$\begin{aligned} \phi &= \phi \\ r &= \sqrt{1 - \cos\theta} \end{aligned} \tag{6}$$

and binned the orientations of the ND bonds into a two-dimensional 50×50 histogram with equal spacing in x and y values between ± 1 where x and y are defined in terms of the projection in the previous equation as

$$x = r\cos\phi \qquad y = r\sin\phi. \tag{7}$$

The resulting pictures (see figure 4) show a view of the bonds from the central N atom.

These histograms can be used to provide a measure of the single-molecule orientational entropy. Suppose the number of occurrences in the ith bin is f_i and the total number in all bins in f_{tot}, then we define the single-particle orientational entropy by

$$S_{orient}/R = \left(\frac{3}{2}\right)\left[-\sum_i \frac{f_i}{f_{tot}} \log \frac{f_i}{f_{tot}} - \log N\right] \tag{8}$$

where N is the number of bins. In the limit of large N this gives a value which is independent of the number of bins. Note that the zero of the entropy defined in this way corresponds to all bins being equally occupied, so the observed values are negative. The histogram does not take into account the three-dimensional nature of the ammonium ion. While the ND bond direction has a distribution in two dimensions, the molecular orientation is defined in three dimensions. The factor of 3/2 in equation (8) is included to take into account the additional degree of freedom.

3. Results: structure

3.1. Variation with temperature

As stated earlier, the distinctive character of the thermal changes in the crystal structure is the onset of an anomalous expansion along the c axis and a contraction of the a axis at temperatures above 150 K. Values of the cell parameters at different temperatures and zero pressure are shown in table 2. Note that atmospheric pressure is $\approx 10^{-3}$ kbar, which is negligible in the context of the computation. In figure 2 we show the same data plotted in a different way. Rather than looking at the values for a and c separately, we show the temperature dependence of the isotropic (ϵ_{iso}) and uniaxial (ϵ_{uni}) strains defined by

$$\begin{aligned} \epsilon_{iso} &= \epsilon_{00} = (\epsilon_{xx} + \epsilon_{yy} + \epsilon_{zz})/\sqrt{3} \\ \epsilon_{uni} &= \epsilon_{20} = (2\epsilon_{zz} - \epsilon_{xx} - \epsilon_{yy})/\sqrt{6} \end{aligned} \tag{9}$$

where

$$\begin{aligned} 1 + \epsilon_{xx} &= a(T)/a(20\,\mathrm{K}) \\ 1 + \epsilon_{zz} &= c(T)/c(20\,\mathrm{K}) \\ \epsilon_{yy} &= \epsilon_{xx}. \end{aligned} \tag{10}$$

The isotropic strain is proportional to the change in volume of the cell, while the uniaxial strain (sometimes called the tetragonal shear strain) measures the elongation (or tetragonal distortion of the cell at *constant volume*. These are the ($L = 0, m = 0$) and ($L = 2, m = 0$) components of the strain tensor expressed as a spherical tensor [18]. We note that the normalization used in equations (9) is different from that used in [9], and that, for practical reasons, we take a low-temperature structure to define the zero of strain.

The top portion of figure 2 shows the temperature variation of these strains in our simulations and in experiments. Experimentally, diffraction experiments show that in the potassium salt the uniaxial strain is about one third of the isotropic strain and both strains increase approximately linearly with temperature. In the ammonium salt (see thin lines in

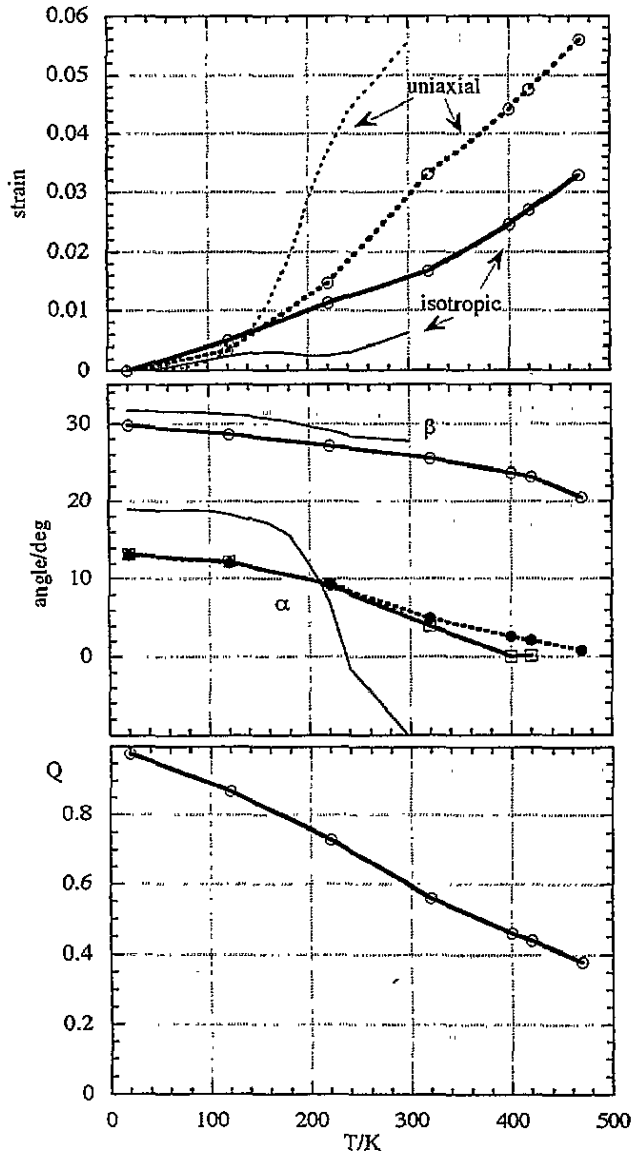

Figure 2. Variation of properties with temperature. The bold lines are for the model; the thin lines are experimental results. Top: uniaxial (dashed) and isotropic strains (solid line). Centre: *angles describing anion (β) and cation (α) orientation. Note that the distribution of cation* orientation becomes very broad. The dashed line shows α_Q, the angle calculated from the order parameters. Bottom: order parameter, $\bar{Q}$.

figure 2) the uniaxial expansion is abnormally large at temperatures above 130 K, while the isotropic strain is lower than expected by comparison with the potassium salt, and even shows a negative coefficient of expansion near 200 K. The results from our simulations are shown by the bold lines in figure 2. The model shows abnormal uniaxial expansion, but spread over a greater temperature range than in the experiment. The isotropic thermal expansion of the model is too large. However, it is less than that in a closely related

model of potassium perrhenate [14] suggesting that although both models are too soft, the differences between them are correct.

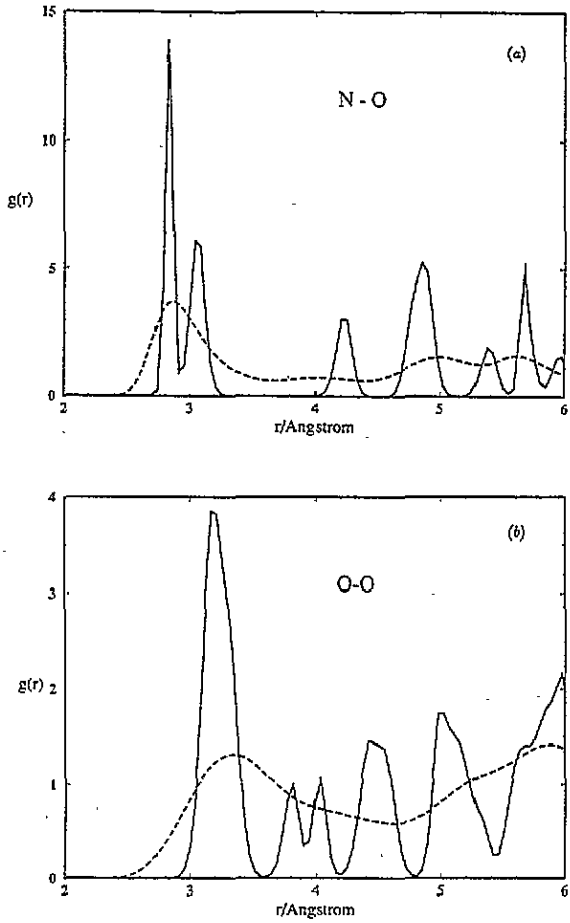

Figure 3. Radial distribution functions at 20 K (solid lines) and 420 K (dashed lines).

Figure 3 shows the radial distribution functions for N–O and O–O at 20 K and at 420 K. At 20 K, the first two peaks in the N–O distribution correspond to the distances from N to the axial and equatorial O atoms. These are clearly separated at 20 K (solid lines), but at 420 K (dashed lines) the two peaks have coalesced into a single broad peak. The N–O, O–O and O–D distances at 20 K agree well with the experimental data ([1]) and give support to the reasonableness of the potential function. The O–D distribution at 420 K is almost featureless, confirming the broad distribution of ammonium-ion orientations. Inspection of the average centre of mass positions confirmed that there was no change of crystal space group throughout the temperature range examined.

Experimentally the angle β of twist of the perrhenate ions has been determined as a function of temperature. This is shown in the central part of figure 2. Good agreement is found between the values in the experiment and in the model, with the correct magnitude of the change with temperature. The mean values of the angle of twist of the ammonium

ions (α) are shown in the same graph. Again the change in the real material is sharper than in our model. However, it must be remembered that as the distribution gets very broad, the mean value of α is less well determined and may differ significantly from the most probable value.

The neutron diffraction data for the ND_4^+ orientation have been interpreted as showing a gradual decrease in the average value of α and an increasingly anisotropic thermal ellipsoid. The spin model suggests that there should be two preferred orientations, the second of which becomes increasingly populated as the temperature is raised, reducing the average value of α. We have looked carefully at the orientational distribution of the ammonium ions in our simulations both by monitoring the order parameters defined in equation (5) and by plotting the two-dimensional histogram of bond orientations. The bottom graph in figure 2 shows plots of the order parameter $\bar{Q}$ as a function of temperature at zero pressure. The values of the α_Q are plotted in the central graph (dashed line). The angles α and the angle determined from the order parameters α_Q agree well and decrease to near zero. Note that although the orientational order as measured by $\bar{Q}$ decreases with temperature, it is still a long way from zero at 420 K, showing that the orientational distribution of the ammonium ions is by no means uniform.

A more detailed picture of the orientational distribution is given in figure 4, which shows a contour plot of the projection of a histogram formed from the N–D bond directions. The projection is constructed in the way described in equations (6) and (7) of section 2 and is formed by taking the upper two ND bonds of ammonium ions in upright sites and inverted molecules in inverted sites. The axes in these figures are chosen to be the same as in figure 1 so the most probable value of α is the angle between a line joining the maxima and a vertical line on the diagram (compare with figure 1). From these plots one can see that the distribution gets much broader as the temperature is raised and the α-values corresponding to the maxima in the distributions decreases. The most significant aspect of these diagrams is that there is no suggestion of two preferred orientations; the axial and equatorial orientations correspond to α-values of $+20°$ and $-50°$ respectively (see figure 3 of [1]).

It is not easy to see directly from these figures that the thermal ellipsoid is anisotropic, as the projection distorts the shape of the distribution away from the zenith. However, we have ascertained that the distribution is elongated by plotting the distribution with the zenith at a different position. However, this elongation is less than is suggested by the neutron data.

The orientational distribution shown in figure 4(d) and the isolated points marked with filled symbols on figure 5 are of particular significance when we come to consider the microscopic basis of the observed changes. They are taken from a run at 420 K in which the cell size and shape were constrained to be the same as at 20 K. The resulting stress is anisotropic with an average value of 6.5 kbar and components 4.0, 3.9 and 11.7 kbar. The probability distribution of the orientation of the ammonium ions is significantly less diffuse than in the zero-pressure run (figure 4(c)) and the maximum in the probability distribution function is $\alpha = +6°$, which is closer to the low-temperature value. This shows that the change in average orientation and some of the spread in orientation is closely connected with the anomalous change in the cell size and shape.

3.2. Variation with pressure

Figure 5 shows the variation of the structural parameters as a function of pressure at constant temperature. The temperature chosen is 420 K, in the anomalous region. As mentioned earlier, the points marked with filled symbols refer to the run with the low-temperature cell whose orientational distribution function was given in figure 4(d).

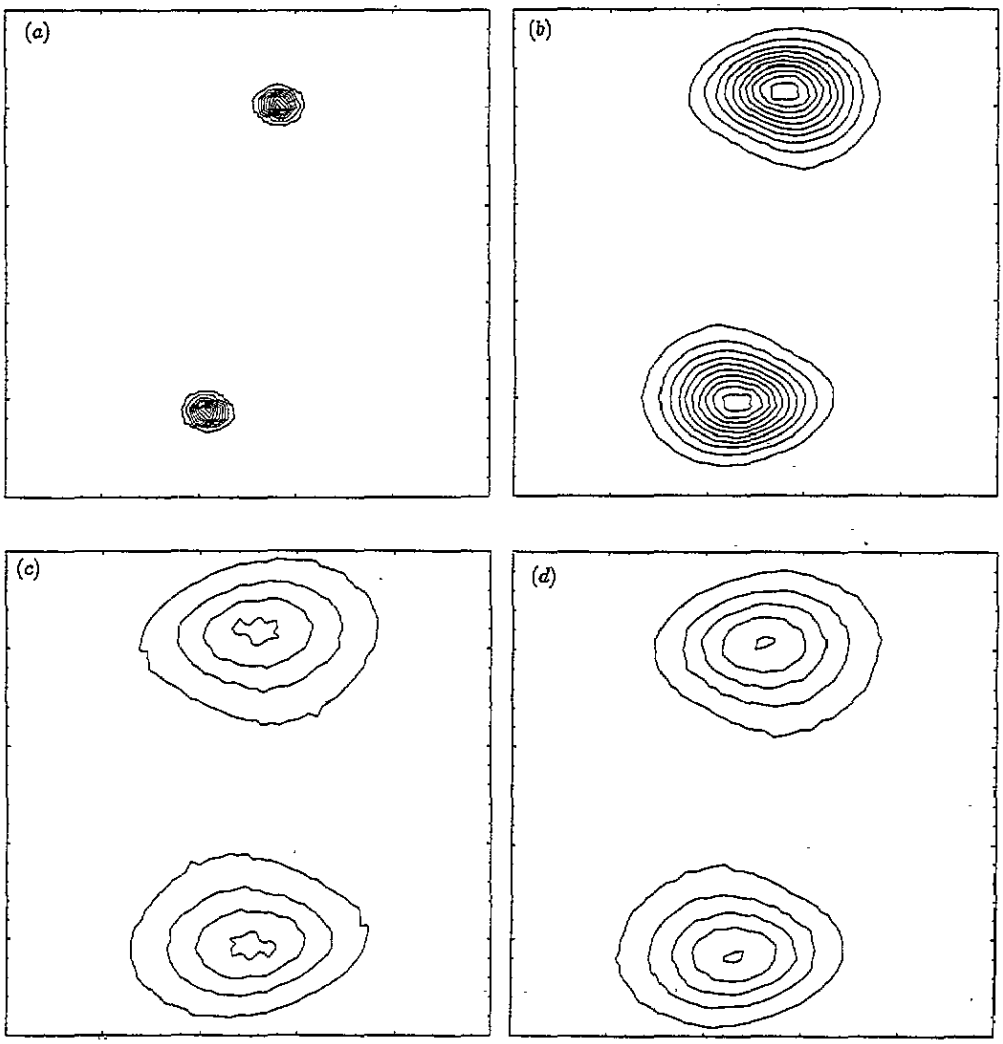

Figure 4. Contour plots of the orientational distribution of the ND bonds. (*a*) 20 K; (*b*) 220 K; (*c*) 420 K; (*d*) low-temperature cell at 420 K. Contours are drawn at the same intervals for the latter three cases. Note how the most probable orientation changes.

There are some differences in the observed behaviour as the pressure is raised compared to the behaviour when the temperature is lowered, although one might expect that increasing pressure would have the same general effect as lowering the temperature. In both cases the angle β describing the ReO_4^--ion orientation increases; however, α, the ammonium-ion orientation parameter, *decreases* and even changes sign as the pressure is increased, although it *increases* as the temperature is lowered. This difference must be related to the change in the uniaxial strain as the temperature changes, compared to the negligible change in this quantity as the pressure changes. We note that several quantities, the energy, ϵ_{uni}, $\bar{Q}$, α_Q and β, go through maximum or minimum values at a pressure of about 10 kbar. We shall find that the orientational entropy and ND_4^+ reorientational correlation times also show extrema at this pressure.

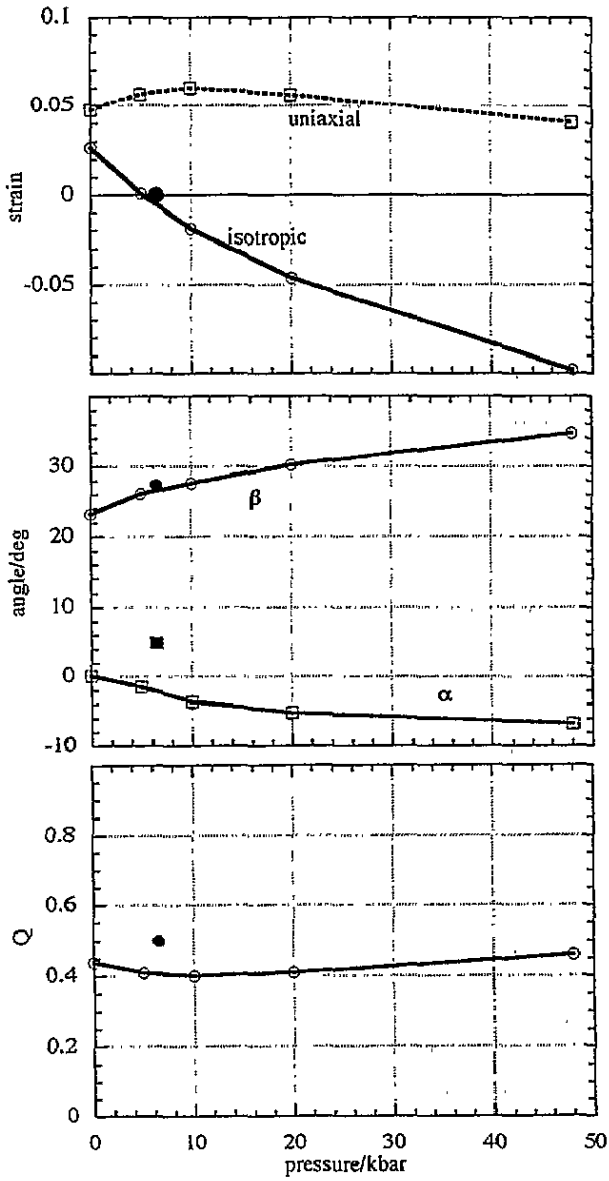

Figure 5. Variation of properties with pressure for the model at 420 K. Isolated solid points show values for the run with the low-temperature cell. Top: uniaxial (dashed) and isotropic strains (solid line). Centre: angles describing anion (β) and cation (α) orientation. Bottom: order parameter, $\bar{Q}$.

3.3. Thermodynamic quantities

The calculated lattice energy of the model at 20 K is -604.4 kJ mol^{-1}. The experimental value for the lattice energy at 298 K is based upon the enthalpies of formation of the gaseous ammonium [19] and perrhenate [20] ions and of the crystalline salt [21] and has the value -629 ± 30 kJ mol^{-1}, showing that our model is less bound than the real material. From runs at 400 K and 420 K at constant (zero) stress and constant strain, the heat capacities

were calculated to be

$$C_\epsilon/R = 12.2 \quad \text{(constant strain)}$$
$$C_\sigma/R = 14.3 \quad \text{(constant stress).} \tag{11}$$

The first value is close to the expected (classical) value of 12 for a crystal containing two rigid non-linear polyatomic ions per formula unit. The difference between the two values ($2.1R$) shows that the energy of deformation makes a significant contribution to the constant-stress heat capacity, as suggested in the analysis of the experimental data [4].

Table 3. Changes in the entropy of of orientational degrees of freedom of ND_4^+ and translational degrees of freedom of both ND_4^+ and ReO_4^- as a function of temperature. These values are relative to the run at 120 K and zero stress. S_{excess} is the entropy in excess of that predicted by applying the harmonic approximation to the crystal at its 120 K structure (see equation (14)).

T/K	P/kbar	S_{orient}/R	$S_{trans,z}/R$	$S_{trans,xy}/R$	S_{excess}/R
120	0	0	0	0	0
220	0	1.2	1.4	0.7	0.5
320	0	2.1	2.3	1.2	1.2
420	0	2.6	3.1	1.6	1.6

The key to understanding the behaviour of the ammonium scheelites must lie in the behaviour of the entropy. At any temperature the Gibbs free energy

$$G = U - ST + \sum_i \sigma_i \epsilon_i \tag{12}$$

is a minimum at constant temperature T and stress components σ_i. The stress–strain contribution, which is analogous to the pV-term for an isotropic material, is negligible at room pressure. The internal energy is a minimum for the low-temperature structure. Hence changes in the structure can be attributed to the increasing importance of the entropy term as the temperature rises. In particular the entropy must change significantly when the material undergoes uniaxial strain. There are two contributions to the entropy that can be measured readily in our simulations, namely the single-particle ND_4^+ orientational entropy and the single-particle translational entropy of both cations and anions. The orientational entropy was estimated from the orientational distribution histograms using equation (8), and changes in the translation entropy by substituting the measured mean square displacements of the centres of mass of the ions into the classical expression for a harmonic oscillator

$$S_{trans}/R = \frac{1}{2}\ln\langle x^2\rangle + \text{constant.} \tag{13}$$

Table 3 shows the variation of the different contributions with temperature. As it is only differences in these values that are significant, these are referred to an energy zero corresponding to the material at 120 K. The last column shows the excess entropy, that is the increase above what one would expect from a harmonic system,

$$S_{excess}/R = \sum S_{trans}/R + S_{orient}/R - D\ln(T/120\,\text{K}) \tag{14}$$

where D is the number of degrees of freedom. As we have included translational contributions from both types of ion and reorientational contributions from the ND_4^+ ions, $D = 9$.

The excess entropy increases during the anomalous expansion, as one would expect. The unexpected result is that changes in the orientational entropy do not dominate the thermodynamics, but are comparable to changes in the translational entropy. Indeed when pressure is applied to the crystal at 420 K, the orientational entropy (shown in table 4) initially increases slightly, reaching a maximum at about 10 kbar. The total entropy for our model must decrease as the pressure is increased or the 0 kbar structure, which is lower in energy than the pressurized structures, would not be stable. One way of seeing this is from the thermodynamic relationship

$$\left(\frac{\partial G}{\partial p}\right)_T = V = \left(\frac{\partial H}{\partial p}\right)_T - T\left(\frac{\partial S}{\partial p}\right)_T \tag{15}$$

which shows that if H decreases with pressure (i.e. becomes more negative, as in our model at 420 K), S must also decrease with pressure. We see from the results in table 4 that the increase in ND_4^+ orientational entropy is outweighed by the reduction in translational entropy due to the decreased amplitudes of the translational motion of both types of ion, that is from the hardening of the phonons.

When one compares the values at 420 K for the zero-stress cell and for the low-temperature cell (see the bottom line of table 4), one finds similar magnitudes for the changes in ND_4^+ orientational entropy and for each of the 6 contributions to the translational entropy. There are other contributions to the entropy which have not been computed, namely the orientational entropy of the ReO_4^- ion and contributions due to correlation of orientation and translational displacement on different ions.

Experimentally the bulk thermal expansion is negative between 160 K and 220 K (see figure 2). From the Maxwell relation

$$\left(\frac{\partial V}{\partial T}\right)_p = -\left(\frac{\partial S}{\partial p}\right)_T \tag{16}$$

we deduce that the entropy *increases* with increasing pressure over this temperature range. Although this phenomenon does not occur in our model which has rather too large a bulk thermal expansion, our results show how this can happen. In the simulations at 420 K we see that the orientational entropy of the ammonium ions initially increases as the pressure is raised from 0 to 5 kbar. In our model this is outweighed by the reduced contributions of the single-particle translations, but the balance is subtle and our results suggest that an increase in disorder of the ammonium ions with pressure must occur in the real material, and must dominate the entropy changes between 160 K and 220 K. As the more ordered form is thermodynamically stable at zero pressure, its energy must increase with pressure to give a minimum free energy in the zero-pressure structure.

4. Results: dynamics

4.1. Reorientation of ammonium ions

Several experiments measure (often indirectly) the rates of reorientation of the ammonium ions. For example, NMR proton relaxation depends on $\tau_{2,\mathrm{HH}}$, the $L = 2$ or dipolar reorientational correlation time of the HH internuclear vector, while the deuteron quadrupolar relaxation in the perdeutero compound depends on $\tau_{2,\mathrm{ND}}$. The Raman line width

of internal modes of the ammonium ion and the rhenium electric quadrupolar relaxation also give information about ammonium-ion reorientation.

In this section we discuss the reorientation of the ND_4^+ ions. We investigated orientational correlation functions

$$C_L(t) = \langle P_L(\cos\theta_R(t)) \rangle \tag{17}$$

where P_L is the Lth Legendre polynomial and $\theta_R(t)$ is the angle between the directions of some vector $\boldsymbol{R}$ at time $t = 0$ and t. We chose three different vectors in the ion, a vector along a ND bond; a vector along a DD bond and a vector along an S_4 axis which bisects the angle between two bonds. As we shall see, the differences between the orientational correlation functions for different vectors give information about the mechanism of jumping. Different experimental techniques probe various aspects of reorientation of different vectors. Experimental results from NMR relaxation, for example, depend on integral relaxation times defined by

$$\tau_{L,\,\mathrm{int}} = \int_0^\infty C_L(t)\ \mathrm{d}t. \tag{18}$$

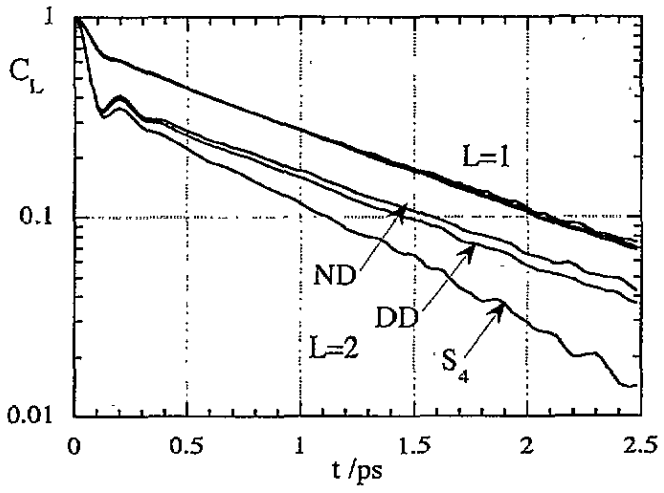

Figure 6. $L = 1$ and $L = 2$ orientational correlation functions for ND, DD and S_4 vectors in an ND_4^+ ion. These are plotted on a logarithmic scale to emphasize the comparison between the different decay rates.

Figure 6 shows the orientational correlation functions for the run at 420 K and zero pressure. These are plotted on a logarithmic scale to emphasize the fact that the asymptotic behaviour is an exponential decay. At short times, however, oscillations can clearly be seen, especially in the $L = 2$ curves (up to about 0.4 ps). After the first 0.4 ps the functions decay exponentially with slopes that are approximately the same for both $L = 1$ and $L = 2$ functions. The slope correlation time, $\tau_{L,\,\mathrm{sl}}$, is defined as the decay constant for

Table 4. Variation of the entropy of the orientational degrees of freedom of ND_4^+ and translational degrees of freedom of both ND_4^+ and ReO_4^- with pressure at 420 K.

T/K	P/kbar	$S(ND_4^+)_{or}/R$	$S_{trans,z}/R$	$S_{trans,xy}/R$	$\sum S/R$
420	0	0	0	0	0
420	5	0.08	−0.6	−0.7	−1.2
420	10	0.09	−0.9	−0.3	−1.1
420	20	0.07	−1.2	−0.4	−1.6
420	48	−0.09	−1.7	−0.6	−2.4
420[a]	(6.5)	−0.23	−0.36	−0.13	−0.72

[a] Run with zero-temperature cell. $p_{xx} = 4.0$ kbar, $p_{zz} = 11.7$ kbar.

the asymptotic exponential decay and was determined by fitting a straight line to the curves of $\ln(C_L(t))$ between $t = 0.4$ and 2.0 ps.

Values for the slope and integral correlation times are given in table 5. There are three main points to notice from figure 6 and the numbers in table 5. First the slope correlation time, which we interpret as the inverse of the rate of jumping between wells, is always longer than the corresponding integral correlation time. Secondly, while the $L = 1$ slope correlation times are shorter than the corresponding $L = 2$ times, the difference is not large. Thirdly, as is apparent in figure 6, the variation in $L = 2$ decay curves for different vectors is greater than the variation for the $L = 1$ curves.

Table 5. Temperature and pressure variation of correlation times (in ps).

T/K	P/kbar	$\tau_{1,sl}$(DD)	$\tau_{1,int}$(DD)	$\tau_{2,sl}$(DD)	$\tau_{2,int}$(DD)	$\tau_{2,sl}$(ND)	$\tau_{2,int}$(ND)	$\tau_{2,sl}(S_4)$	$\tau_{2,int}(S_4)$
220	0	15.8	14.2	14.8	10.9	14.9	11.1	9.8	7.4
320	0	2.38	1.92	2.3	1.29	2.4	1.4	1.6	0.99
420	0	1.05	0.77	1.02	0.46	1.08	0.49	0.76	0.35
420	5	0.82	0.60	0.83	0.35	0.86	0.38	0.72	0.29
420	10	0.75	0.54	0.77	0.31	0.77	0.33	0.61	0.25
420	20	0.72	0.53	0.70	0.32	0.70	0.33	0.55	0.25
420	48	0.90	0.63	0.90	0.40	0.91	0.43	0.94	0.35
420[a]	(6.5)	1.68	1.27	1.57	0.81	1.66	0.86	1.31	0.65
420[b]	0	0.87	0.62	0.85	0.37	0.90	0.40	0.74	0.31

[a] Run with zero-temperature cell. $p_{xx} = 4.0$ kbar, $p_{zz} = 11.7$ kbar.
[b] Run with NH_4^+ in place of ND_4^+.

One can deduce quite a bit about the librational and reorientational motion of the ammonium ions from figure 6 and the comparable functions at different temperatures. At 20 K and 120 K the $L = 1$ and $L = 2$ orientational correlation functions do not decay to zero as, on the time scale of the simulation, the ammonium ions do not move between equivalent energy minima. The initial decay is due to librational motion in the well. At 420 K the remnants of this librational motion can be seen at short times, but at longer times the correlation functions decay to zero as the molecules move from one potential well to an equivalent one. This jumping between wells determines the 'slope correlation time', defined as the inverse of the asymptotic decay rate. The reason that there is more difference between the slope correlation times and the integral correlation times for the $L = 2$ functions than

the $L = 1$ functions is that the initial decay of the P_2-function due to libration within a well is greater than the decay of the P_1-function.

In the limit of Debye diffusion, where the distribution is assumed to be uniform and the jumps in orientation are assumed to be small, the slope correlation times would be the same for all vectors and would satisfy $\tau_1 = 3\tau_2$. Here we see differences between vectors (at least for the $L = 2$ correlation functions), but little or no difference between the slope correlation times for $L = 1$ and $L = 2$ functions. Clearly the Debye diffusion model is inapplicable, which is not surprising given that there is a strongly preferred orientation. We can use the variation between different vectors to deduce something about the mechanism of reorientation. If the ions reorient at a rate τ^{-1} by jumps of 120° about the C_3 axes along bonds, one expects (see appendix for details of the derivation)

$$\begin{aligned} &P_1(\cos\theta) = \exp[-t/\tau] \qquad \text{all vectors} \\ &P_2(\cos\theta_{ND}) = \exp[-t/\tau] \\ &P_2(\cos\theta_{DD}) = 0.75\exp[-t/\tau] + 0.25\exp[-1.5t/\tau] \\ &P_2(\cos\theta_Z) = \exp[-1.5t/\tau] \end{aligned} \tag{19}$$

while if reorientation is by jumps of about 180° about the X, Y or Z axes of the ion, then all vectors and L-values relax at the same rate. The observed differences suggest that most reorientational jumps are C_3 in character.

Table 6. Activation energies for reorientation in kJ mol^{-1}.

Vector	$L = 1$ (slope)	$L = 2$ (slope)	$L = 1$ (integral)	$L = 2$ (integral)
DD	10.5	10.4	11.4	12.5
ND	10.5	10.1	11.4	12.2
S_4	9.9	9.5	10.8	11.5

The apparent activation energies calculated from the observed values of the correlation times are given in table 6. The value for the $L = 2$ integral correlation time is in reasonable agreement with the value of 9.3 kJ mol^{-1} observed experimentally from NMR [7].

We also observed the variations in these relaxation rates with pressure, and the results are also given in table 5. Surprisingly, up to pressures of about 10 kbar the rates increased and then decreased at higher pressures. This is consistent with our observation of a maximum orientational disorder at 10 kbar. Experimentally [22] the proton T_1 decreases slightly with pressure showing that the motion is slowed on applying pressure at room temperature. The pressure dependence of the correlation time is

$$RT\frac{\partial \ln \tau_C}{\partial p} = 1.4\,\text{cm}^3\ \text{mol}^{-1} \tag{20}$$

at room temperature. We predict that between 150 K and 220 K where the bulk thermal expansion is negative, and as we have seen the entropy increases with pressure, T_1 will be found to *increase* with pressure.

The results discussed so far are for the deutero salt; comparable values for the NH_4^+ salt are given in the bottom line of table 5 from a simulation at 420 K and zero pressure. In this salt the decay rate for cation reorientation is faster for NH_4^+ than ND_4^+ by a factor of about 10%. If the process depended only on the rotational motion of the ion itself, one would expect a ratio of $\sqrt{2}$, as the ratio of the moments of inertia is equal to 2. This suggests that other degrees of freedom such as translational phonons also affect the orientational decay.

Table 7. Frequencies of zone-centre modes in cm^{-1}. R and T denote librational and translational modes respectively.

Symmetry	Assignment	Frequency (model)	Frequency (experiment)
B_g	ReO_4^- T	47	49
E_g	ReO_4^- T	73	67
E_u	ReO_4^- R	98	
A_g	ReO_4^- R	94?	134
E_g	ND_4^+ T	101?	117
E_u	TO	163	
B_u	ReO_4^- R	114	
E_g	ReO_4^- R	161	174
B_g	ND_4^+ T	256	193
A_g	ND_4^+ R	207	
E_g	ND_4^+ R	211?	

4.2. *Spectroscopy*

We have measured the zone-centre frequencies by Fourier transforming collective time correlation functions of the linear velocity

$$C_{v\Gamma} = \left\langle \sum_i \gamma_i v_{i\alpha}(0) \sum_j \gamma_j v_{j\alpha}(t) \right\rangle \tag{21}$$

and a corresponding function for the angular velocity. In this expression $v_{i\alpha}$ is the velocity on the centre of mass of the ith ion in direction α and $\gamma_i = \pm 1$ is a constant whose value depends on the symmetry of the mode. For g modes it is equal to +1 for upright sites and to −1 for inverted sites, while for u modes it is equal to +1 at all sites. The correlation functions for ammonium and perrhenate ions were calculated separately. x and y linear and angular velocity components give degenerate modes, while the z velocity component gives non-degenerate modes. The values of the frequencies we determined in this way from the simulation at 20 K are given in table 7 together with the experimental values. In some cases (marked with queries) the assignment was not certain due to the possible presence of combination bands in our spectra.

The most interesting point about the correlation functions is their change with temperature. At 420 K the correlation functions for the perrhenate motion are very similar to those at 20 K, but those for the ammonium-ion motion are strongly damped, decaying to zero by 0.5 ps (angular velocity) or 0.8 ps (linear velocity). This is illustrated in figure 7 where the single-particle ND_4^+ velocity and angular velocity correlation functions are shown at 20 K and 420 K. At the higher temperature the angular velocity correlation functions are strongly damped by the ammonium-ion reorientation, and most of the phonon structure is lost. A similar effect is seen in the linear velocity autocorrelation functions, showing that there must be considerable coupling between the translational and reorientational motion of the ND_4^+ ions. On the other hand the changes in the ReO_4^- motion are much less, and similar to those seen in normal crystals. This implies that phonons involving librational and translational motion of the ND_4^+ ions are very broad, whilst those involving ReO_4^- -ion motion remain reasonably sharp and well defined. This is entirely consistent with the observation that in a Raman spectrum the external ammonium modes broaden and disappear as the anomalous temperature is reached [5].

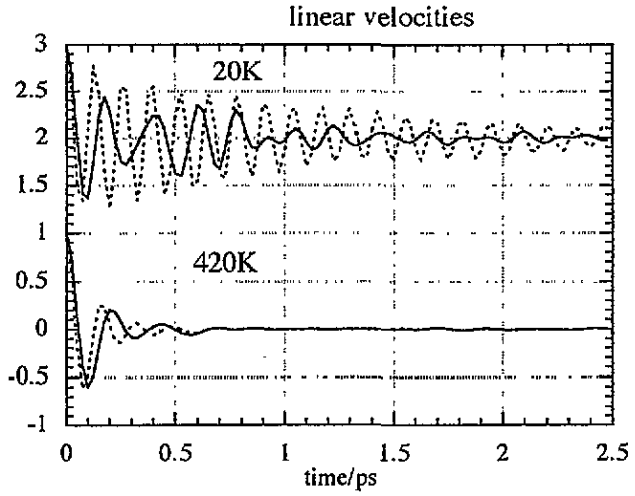

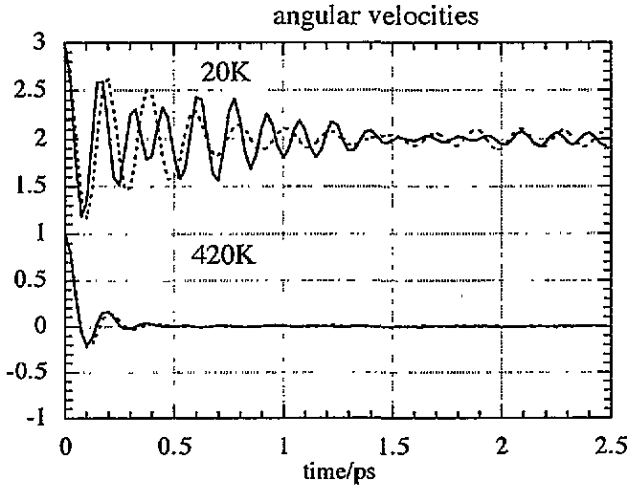

Figure 7. ND_4^+ single-particle velocity and angular velocity–time correlation functions at 20 K and 420 K. Note the rapid damping at the higher temperature. Full lines: x and y components; dashed lines: z components.

4.3. Quadrupolar relaxation of rhenium

Nuclear quadpupolar relaxation provides a probe for motion in liquids and solids. The rate of relaxation is proportional to

$$\langle V_{\pm m} V_{\mp m} \rangle j(\omega_m) \tag{22}$$

where V_m is the mth spherical component of the electric field gradient tensor and $j(\omega_m)$ is the spectral density of the fluctuations in V_m at frequency ω_m. These frequencies, which correspond to the energy differences btween Re quadrupolar levels, are small ($\approx$ 30 MHz).

In a crystal one can expand V_m in powers of the phonon displacement coordinates q_k:

$$V_m - V_m^0 = \sum_k \frac{\partial V_m}{\partial q_k} + \frac{1}{2}\sum_{k,k'} \frac{\partial^2 V_m}{\partial q_k \partial q_{k'}} + \ldots . \tag{23}$$

In an ordered crystal the effect of the first term (the harmonic term) in this equation is smaller than the second, as the spectral density of fluctuations of the first term is just the phonon density of states at ω_m, which is small as it is proportional to ω_m^2/ω_D^2 where ω_D is the Debye frequency of the crystal, while the spectral density of the second term is much greater as it involves Raman-like processes in which one phonon is created and another destroyed [23]. As a result at high temperatures the relaxation rate increases as the square of the temperature rather than linearly with temperature, as would be predicted from the harmonic term.

It has been shown that the increase of relaxation rate of the NQR resonance of Re in ammonium perrhenate between about 100 K and 250 K is more rapid than the T^2-dependence expected for phonon relaxation [24]. The additional relaxation mechanism is thought to be due to fluctuations in the electric field gradient at the Re atom caused by changes in the orientation of the ammonium ion. This could be the result of a greatly increased amplitude of the fluctuations due to the change in orientational distribution function of the ammonium ions, or to an increase in the spectral density, or to both. We have attempted to investigate these factors, but have found some problems in doing so.

For each Re atom, the EFG was calculated using a point charge model for the ammonium ion with atomic charges equal to those assumed in the potential energy function (table 1). Since the lowest electric moment of the ammonium ion is the octupole moment, the external electric field gradient decreases with distance as R^{-6} and only the eight nearest ammonium ions around each perrhenate ion need be included in the sum.

The point charge contributions to the cartesian components of the EFG tensor were calculated from the formula

$$V_{\alpha\beta} = \left(\frac{e}{R^5}\right)\{3X_\alpha X_\beta - \delta_{\alpha\beta}R^2\}. \tag{24}$$

The autocorrelation functions of the spherical components were calculated from the formulae

$$\begin{aligned} \langle V_{\pm 1}(0)V_{\mp 1}(t)\rangle &= \langle V_{zx}(0)V_{zx}(t)\rangle + \langle V_{zy}(0)V_{zy}(t)\rangle \\ \langle V_{\pm 2}(0)V_{\mp 2}(t)\rangle &= \frac{1}{4}\langle [V_{xx}(0) - V_{yy}(0)][V_{xx}(t) - V_{yy}(t)]\rangle + \langle V_{xy}(0)V_{xy}(t)\rangle \end{aligned} \tag{25}$$

in which the imaginary parts have been omitted as they average to zero [25].

Table 8. Mean square fluctuations in the tensor components of the electric field gradient at a rhenium nucleus. Units are 10^{-5} electrons^2 Å^{-6}.

T/K	$\langle V_{-1}V_{+1}\rangle$	$\langle V_{-2}V_{+2}\rangle$
20	0.3	0.3
120	1.8	1.8
220	3.3	3.5
320	4.9	5.7
420	6.4	7.8

The mean square amplitudes of the fluctuations of V_1 and V_2 are shown in table 8. $\langle V_{+1}V_{-1}\rangle$ increases approximately linearly with temperature, and $\langle V_{+2}V_{-2}\rangle$ slightly more rapidly. These values include both the linear and the quadratic terms in equation (23) and are probably dominated by the linear term, which we have argued is less important for nuclear quadrupolar relaxation in normal crystals with small amplitudes of motion.

Some information about changes in spectral densities at low frequencies can be found from the velocity and angular velocity correlation functions shown in figure 7. As these are single-particle correlation functions, their Fourier transforms give the phonon density of states of the corresponding motion (translation or libration). The onset of reorientation of the ND_4^+ ions between different (but equivalent) sites dampens both the angular and linear velocity correlation functions for the ND_4^+ ions, leading to a greatly increased density of states at zero and low frequencies (sometimes known as a diffusional peak). A crystal, such as this, which has reorientational motion has a spectral density which is intermediate between a liquid at a high temperature, where the maximum spectral density (equal to $2\tau_C$) is at zero frequency and a Debye crystal where the maximum spectral density is at the Debye frequency.

In principle this provides an explanation of the increased quadrupolar relaxation rate in the anomalous region, namely that the increased spectral density at the quadrupolar frequencies due to the diffusional peak increases the contribution of the first (harmonic) term in equation (23), giving an increased relaxation rate.

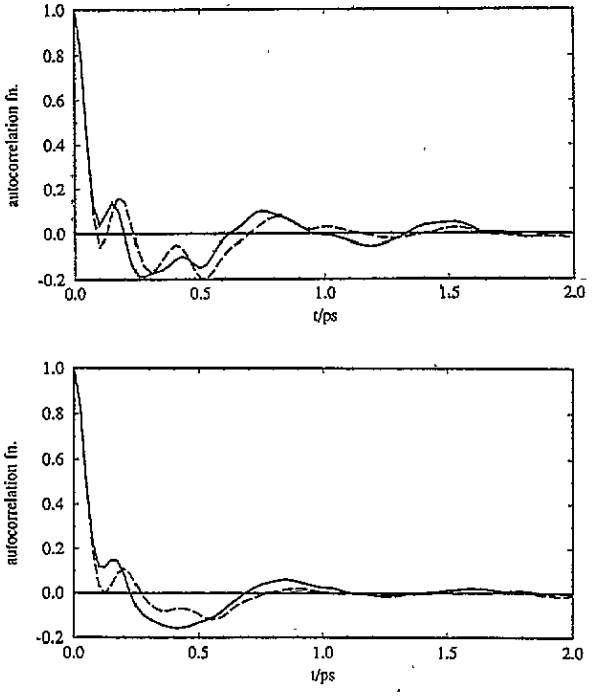

Figure 8. Time correlation functions for the $m = 1$ (solid lines) and $m = 2$ (dashed lines) components of the electric field gradient tensor at a rhenium nucleus. Above: 220 K; below: 420 K.

In order to find some more direct evidence for this argument, we examined the time

correlation functions for the components of the electric field gradient. Figure 8 shows these functions at 220 K and 420 K. At both temperatures the functions rapidly drop to zero and then fluctuate about that value. If we could be sure that these fluctuations had died out by 2 ps, then we could estimate $j(0)$ by taking the integral under the curve as is done in simulations of liquids. However, this is not valid at 220 K and probably not at 420 K, so we cannot estimate the spectral densities at zero and very low frequencies. The fluctuations in these functions contain oscillations due to both the motion of the ammonium ions and the slower translational motion of the perrhenate ions. The latter oscillations persist at all temperatures, although some of the faster oscillations due to the ammonium-ion reorientation disappear at the higher temperatures. The result is that there is little change in the shape of the correlation functions as the temperature is changed.

4.4. Conclusions

The qualitative agreement between the results of this model and the experimental observations is satisfactory. The model shows anomalous expansion, onset of NH_4^+ reorientation and changes in the average NH_4^+ orientation as the temperature is raised. Quantitatively some aspects are less satisfactory, in particular the anomalous expansion and associated phenomena are spread out over a wider temperature range than in the real material. As in our earlier study of the potassium salt we find that the thermal expansion is overestimated. It seems, however, that our model is sufficiently realistic to contain the essential physics of the material and we can now consider what insight we have gained into the microscopic basis of the thermal behaviour of the ammonium scheelites.

The most important microscopic quantity is the orientational distribution of the NH_4^+ or ND_4^+ ions. As the temperature is raised, this becomes broader and shifts, so the preferred direction of the ND bonds becomes closer to being aligned in the *ac* and *bc* planes. However, even at the highest temperature investigated the orientational distribution function is significantly non-uniform, as shown both by the contour diagrams of the orientational distribution and in the value of the mean order parameter, $\bar{Q}$ which drops from 0.98 at 20 K to 0.44 at 420 K. If the orientational distribution were completely uniform the value of $\bar{Q}$ would be zero. This non-uniform distribution with a single preferred orientation is consistent with the neutron scattering data, but not in accord with the pseudo-spin model. Compared to the neutron data, the distribution of angles around the crystal *c* axis (α) is probably not broad enough.

Although the time scale for molecular reorientation of the ND_4^+ ions is remarkable short at 320 K and above (1 ps) it is not correct to think of the ions as freely rotating. Rather they are librating within an orientational potential well and moving between such wells. There are 12 wells which are equivalent except for the labelling of the nuclei. By examining the correlation times for different vectors and different *L*-values, we were able to deduce that the principal mechanism for the ion to move between these wells is by jumps of approximately 120° about a bond direction. All the time correlation functions show a rapid initial decay with some oscillations followed by exponential decay at longer times. The first part of the decay can be attributed to motion within a well, while the exponential decay gives information about the rate of jumping between wells.

This study shows that the integral relaxation time (probed in magnetic resonance experiments) has contributions from both the short- and long-time decay processes and so should not be interpreted as giving the rate of jumping between wells. It is also inappropriate to deduce a rotational diffusion constant as the motion is not diffusional, but includes large angular jumps between equivalent wells. Our calculations show that there may be small

differences (about 5%) between the $L = 2$ reorientational correlation times of the ND bond (probed in deuteron relaxation experiments) and the HH bond (probed in proton relaxation).

The final question to be addressed is why the ammonium scheelites exhibit anomalous expansion. Here it is useful to compare the ammonium and potassium salts as, if the ammonium ion were spherical, one would expect approximately the same ratio of c to a as in the potassium salt. This ratio is 2.222 at 15 K and increases to 2.237 at 300 K. For ammonium perrhenate the experimentally observed ratio increases from 2.066 at 20 K where the ammonium ion is most localized, to 2.208 at 300 K. Thus at high temperatures the ratio increases towards the value expected for an effectively spherical ion. Now as the temperature is lowered the ammonium ions become more localized and point at the axial O atoms, pulling them closer. As these ions are on the ReO_4^- ions in the planes above and below the NH_4^+ ion (see figure 1) this causes the c axis to shrink more than the a axis. Thus we can interpret the anomalous expansion as resulting from the swing of the preferred ammonium ion orientation from $\alpha = 13°$ where they interact with the axial O atoms belonging to anions in the planes above and below to $\alpha \approx 0°$ where they interact with both the axial atoms from the planes above and below and the equatorial atoms from the ions in the same plane. This pulls these ions closer resulting in a contraction of the lattice vector a, while at the same time c expands.

Why does this happen? To attempt to answer this question it is constructive to compare the results from the simulation at 420 K using the low-temperature cell with the simulation at the same temperature with the elongated cell that gives zero stress. At this temperature the internal energy is lower in the low-temperature cell by 2.9 ± 0.2 kJ mol^{-1}. The stability of the elongated cell must be due to an increase in entropy of at least $0.83R$. In our investigation of the single-particle contributions to the entropy in our model we found that some of this comes from the increased single-particle orientational entropy, but as much comes from the increased amplitude of vibration of the ions from their equilibrium positions.

Finally we return to the question as to what we have learned about the real material from this study. We recognize that simulation of a model system is not the same as investigating the behaviour of a real system. We cannot rule out the possibility that, unlike in our model, the real material does have two possible NH_4^+ orientations. However, the results from the model show that this is not a prerequisite for anomalous thermal expansion and suggest that new experimental investigations are needed.

Acknowledgments

We thank Dr I R McDonald for helpful discussions and both him and Dr M Ferrario for use of their molecular dynamics program. We are grateful to NSERC (Canada) for an operating grant to RJCB, the British Council for support for a sabbatical visit of RJCB and to SERC for computational support (grant GR/H/04190).

Appendix. Jump models for reorientation

The tetrahedral ammonium ion at a given site has 12 equivalent molecular orientations related to each other by rotations of the molecule between orientations which are only distinguishable by the labelling of the nuclei. In this appendix we derive orientational relaxation rates for various vectors in the ion for two models of jumping between orientations. In the first model the ion jumps by $\pm 120°$ about one of the bond directions

Table A1. Values of angles and Legendre polynomials for various vectors in the ND_4^+ ion. θ_T is the tetrahedral angle (=109.47°).

	(12)	(13)	(14)	(23)	(24)	(34)	(43)	(42)	(32)	(41)	(31)	(21)
$\theta_{ij:12}$(DD)	0°	60°	60°	60°	60°	90°	90°	120°	120°	120°	120°	180°
$P_1(\theta_{ij:12}$(DD))	1	1/2	1/2	1/2	1/2	0	0	−1/2	−1/2	−1/2	−1/2	−1
$P_2(\theta_{ij:12}$(DD))	1	−1/8	−1/8	−1/8	−1/8	−1/2	−1/2	−1/8	−1/8	−1/8	−1/8	−1
$\theta_{ij:12}(S_4{-}z)$	0°	90°	90°	90°	90°	180°	180°	90°	90°	90°	90°	0°
$\theta_{ij:12}(S_4{-}x)$	0°	90°	90°	90°	90°	0°	180°	90°	90°	90°	90°	180°
$P_1(\theta_{ij:12}(S_4{-}z))$	1	0	0	0	0	−1	−1	0	0	0	0	1
$P_1(\theta_{ij:12}(S_4{-}x))$	1	0	0	0	0	1	−1	0	0	0	0	−1
$P_2(\theta_{ij:12}(S_4))$	1	−1/2	−1/2	−1/2	−1/2	1	1	−1/2	−1/2	−1/2	−1/2	−1
$\theta_{ij:12}$(ND)	0°	0°	0°	θ_T	θ_T	θ_T	θ_T	θ_T	θ_T	θ_T	θ_T	θ_T
$P_1(\theta_{ij:12}$(ND))	1	1	1	−1/3	−1/3	−1/3	−1/3	−1/3	−1/3	−1/3	−1/3	−1/3
$P_2(\theta_{ij:12}$(ND))	1	1	1	−1/3	−1/3	−1/3	−1/3	−1/3	−1/3	−1/3	−1/3	−1/3

chosen at random (C_3 jumps), while in the second model the ion jumps by 180° about on of the three S_4 axes.

Consider a cube with the H atoms at corners (111), (1−1−1), (−11−1), (−1−11). The atoms are labelled by $j = 1$–4, and any orientation is uniquely specified by the pair of labels of the atoms on the top of the cube, i.e. at the corners (111) and (−1−11). If $p(i, j)$ is the probability of finding orientation (i, j), then its rate of change is given by the master equation

$$\frac{\mathrm{d}}{\mathrm{d}t}p = k\mathbf{R}p \tag{A1}$$

where $\mathbf{R}$ is the jump matrix with dimension 12×12 and k is the rate of jumping. This can be integrated to give

$$p(t) = \exp[k\mathbf{R}t]p(0). \tag{A2}$$

For C_3 jumps there are eight possible outcomes with equal probability, giving the following matrix elements of $\mathbf{R}$:

$$\begin{aligned} R_{ij,ij} &= -1 \\ R_{ij,ik} &= R_{ij,ki} = R_{ij,kj} = R_{ij,jk} = 1/8 \\ R_{ij,jl} &= R_{ij,kl} = 0. \end{aligned} \tag{A3}$$

The eigenvalues and eigenvectors of this matrix are readily found to be

$$
\begin{aligned}
0 \quad & (1/\sqrt{12})\{(12) + \text{all other permutations}\} \\
-1.5 \quad & (1/\sqrt{24})\{[2(12) + 2(34) - (13) - (24) - (14) - (23)] \\
& + \text{a similar term with } (ij) \text{ for } (ji)\} \\
-1.5 \quad & (1/\sqrt{8})\{[(13) + (24) - (14) - (23)] \\
& + \text{a similar term with } (ij) \text{ for } (ji)\} \\
-1.0 \quad & (1/\sqrt{4})\{[(12) - (34)] \\
& + \text{a similar term with } (ij) \text{ for } (ji)\} \\
-1.0 \quad & (1/\sqrt{4})[(12) - (21)] \\
-1.0 \quad & (1/\sqrt{4})[(34) - (43)] \\
-1.0 \quad & (1/\sqrt{4})[(13) - (31)] \\
-1.0 \quad & (1/\sqrt{4})[(24) - (42)] \\
-1.0 \quad & (1/\sqrt{4})[(14) - (41)] \\
-1.0 \quad & (1/\sqrt{4})[(23) - (32)].
\end{aligned}
\tag{A4}
$$

The required correlation functions are

$$\langle P_L(\cos(\theta(t))) = \sum_{ij} p_{ij}(t) P_L(\theta_{ij:12}) \tag{A5}$$

where $p_{ij}(t)$ is obtained from equation (27) with the initial condition that the ion is aligned in the (12) orientation at time $t = 0$ and $\theta_{ij:12}$ is the angle moved by the vector concerned when the ion reorients from the (12) position to the (ij) position. Table A1 shows these angles and the corresponding values of the Legendre polynomials for a DD vector, the S_4 vectors in the z and x directions, and for a vector along a ND bond. From this table and the eigenvectors of the jump matrix in equation (29) we deduce that for C_3 jumps about bond directions

$$
\begin{aligned}
& P_1(\mathrm{DD}) = P_1(\mathrm{ND}) = P_1(\mathrm{S_4}) = \exp[-t/\tau] \\
& P_2(\mathrm{DD}) = 0.25\exp[-1.5t/\tau] + 0.75\exp[-t/\tau] \\
& P_2(\mathrm{S_4}) = \exp[-1.5t/\tau] \\
& P_2(\mathrm{ND}) = \exp[-t/\tau].
\end{aligned}
\tag{A6}
$$

For random jumps about the three S_4 axes the jump matrix is different. It has only two distinct eigenvalues, 0 and –4/3, so all L correlation functions for any vector decay at 4/3 of the jump rate. The fact that we observe different decay rates for different vectors supports the idea that jumps occur by 120° about a bond direction.

References

[1] Powell B M, Brown R J C, Harden A M C and Reid J K 1993 *Acta Crystallogr.* B 49 463

[2] Brown R J C, Powell B M and Stuart S N 1993 *Acta Crystallogr.* C **49** 214
[3] Weir R D and Staveley L A K 1980 *J. Chem. Phys.* **73** 1386
[4] Brown R J C, Callanan J E, Weir R D and Westrum E F 1986 *J. Chem. Phys.* **85** 5963
[5] Korppi-Tommola J, Devarajan V, Shurvell H F and Brown R J C 1978 *J. Raman Spectrosc.* **7** 96
[6] Park Y S, Brown R J C and Shurvell H F 1986 *J. Raman Spectrosc.* **17** 351
[7] Armstrong R L, Lourens J A J and Jeffrey K R 1976 *J. Magn. Reson.* **23** 115
[8] Brown R J C and Segel S L 1977 *J. Chem. Phys.* **67** 3163
[9] Taylor D R 1987 *J. Chem. Phys.* **87** 773
[10] Taylor D R 1989 *Phys. Rev.* B **40** 493
[11] Lynden-Bell R M, Ferrario M, McDonald I R and Salje E 1989 *J. Phys.: Condens. Matter* **1** 6523
[12] Ferrario M, Lynden-Bell R M and McDonald I R 1994 *J. Phys.: Condens. Matter* **6** 1345
[13] Fowler P W, Kelly H M and Brown R J C 1993 *Chem. Phys. Lett.* **216** 200
[14] Brown R J C, Lynden-Bell R M, McDonald I R M and Dove M T 1994 *J. Phys.: Condens. Matter* **6** 9895
[15] Allen M P and Tildesley D J 1987 *Computer Simulation of Liquids* (Oxford: Oxford University Press)
[16] Lynden-Bell R M and Michel K H 1994 *Rev. Mod. Phys.* **66** 721
[17] Lynden-Bell D 1987 *Q. J. R. Astron. Soc.* **28** 187
[18] Zare R N 1988 *Angular Momentum* (New York: Wiley)
[19] Johnson D A 1988 *J. Chem. Soc.: Dalton Trans.* 445
[20] Sidorov L N, Rudnyi E B, Nikitin M I and Sorokin I D 1983 *Dokl. Akad. Nauk. SSR (Phys. Chem.)* **272** 1172
[21] Johnson D A 1990 *J. Chem. Soc.: Dalton Trans.* 3301
[22] Mackowiak M and Brown R J C 1983 *J. Mol. Struct.* **111** 233
[23] Abragam A 1961 *Principles of Nuclear Magnetism* (Oxford: Oxford University Press)
[24] Szabo A J and Brown R J C 1994 *Z. Naturf.* a **49** 302
[25] Slichter C P 1990 *Principles of Magnetic Resonance* 3rd edn (Berlin: Springer)